Optical extinction properties of carbon onions prepared from diamond nanoparticles

Satoshi Tomita*
Nanomaterial Processing Laboratory, RIKEN, Hirosawa, Wako, Saitama 351-0198, Japan

Minoru Fujii and Shinji Hayashi
Department of Electrical and Electronics Engineering, Faculty of Engineering, Kobe University, Rokkodai, Nada, Kobe 657-8501, Japan
(Received 11 June 2002; revised manuscript received 20 September 2002; published 31 December 2002)

Optical extinction due to surface plasmon resonances of spherical and polyhedral carbon onions prepared from diamond nanoparticles has been studied. Extinction spectra for the onions dispersed in the distilled water were obtained experimentally by optical transmission spectroscopy. Theoretical considerations were given to interpret the experimental results. For spherical onions, a defective spherical onion model was introduced and the experimental extinction features were traced back to the aggregate of the defective spherical onions. The extinction spectrum with two peaks for the aggregate of polyhedral onions was reproduced by treating the planar segments of the onions as ellipsoidal graphite nanocrystals with crystalline anisotropy. The present study may allow us to address a long-standing important problem about an origin of the interstellar extinction bump.

DOI: 10.1103/PhysRevB.66.245424 PACS number(s): 78.67.Bf, 81.05.Tp

I. INTRODUCTION

The discovery of C_{60}[1] has stimulated intensive research efforts on cagelike carbonaceous nanomaterials, so-called fullerenes. Owing to their intriguing properties, fullerenes are believed to play an important role at the cutting edge of nanoscience and nanotechnology. In 1992 a new member of the fullerene family, named carbon onions, was reported by Ugarte.[2] Carbon onions are zero-dimensional carbonaceous nanoparticles in the size ranging from a few to several tens nanometers. They consist of concentric curved graphitic shells with an interlayer distance of 0.34 nm, which is close to that of bulk graphite, and look like onions. Since the onion structures are considered to be favored over the planar graphite-like structures and energetically stable,[3] carbon onions offer a good model system to study optical and dielectric properties of graphitic nanoparticles in zero dimension.[4–7]

In sufficiently small spheres, such as graphitic nanoparticles, with the dielectric function $[\epsilon(\omega)]$ of frequency ω placed in the surrounding medium with the dielectric constant (ϵ_m), a surface mode (Fröhlich mode) is excited at the frequency ω_F, where $\epsilon(\omega_F)=-2\epsilon_m$ is satisfied.[8] The surface plasmon excitation is accompanied by the absorption of electromagnetic wave. Lucas and co-workers[9] theoretically demonstrated that carbon onions with core materials in vacuum medium show an absorption peak due to the surface plasmon around 4.6 μm^{-1} (217.5 nm, 5.7 eV). Interestingly, their calculation predicted that the peak position and width depend on the ratio of inner core radius r to graphitic shell radius R of the onions.

From experimental point of view, there has been a few works on optical extinction properties of carbon onions. de Heer and Ugarte[10] reported that water suspensions of polyhedral onions with empty cores, which are prepared by annealing carbon soot, exhibit an extinction peak at 3.8 μm^{-1}. The heavy redshift of the surface plasmon resonance was tentatively explained by the water environment, clustering effect,[9] and effect of elongation of the onions.[11] Carbon onion thin films produced by an ion implantation technique are reported to show two extinction peaks.[12] The peaks at 4.3 and 3.8 μm^{-1} are likely to be attributed to absorption by carbon onions and graphitic residues in the voids between the onions, respectively. In spite of these pioneering works, the optical extinction properties of the onions are still a matter for debate. In particular, little is known about the shift variation of the extinction peak by changing the geometrical factor r/R of an onion. A systematic experimental study combined with theoretical considerations for the extinction properties of the onions is thus highly desired in the context of physics and material science.

Recently, we have prepared carbon onions in a large quantity by annealing diamond nanoparticles in vacuum.[13] With increasing the annealing temperature, diamond nanoparticles are transformed into onions. The transformation proceeds from the surface to the center in each diamond.[14,15] Owing to the transformation mechanism, the particles at the intermediate stage of the transformation have core-shell structures, where shells and cores are graphitic layers and diamonds, respectively;[16] the r/R of the onions can be varied by changing annealing temperature in this system. The structure and electronic properties of the onions have already been investigated using transmission electron microscopy (TEM), electron energy-loss spectroscopy (EELS),[13] electron spin resonance (ESR),[17] and synchrotron x-ray diffraction.[18] The purpose of this study is to build up a knowledge on optical extinction properties of the onions. We experimentally obtain extinction spectra of the onions. The results are interpreted semiquantitatively by theoretical considerations based on the onion models that are newly constructed.

Finally yet importantly, the optical extinction at about 4.6 μm^{-1} by the onions in vacuum has attracted great interest also from the viewpoints of astronomy and astrophysics. Astronomers have observed an extinction bump of star light at 4.6 μm^{-1} caused by interstellar dust.[19,20] Although many models of the dust particles have been constructed,[21–25] they

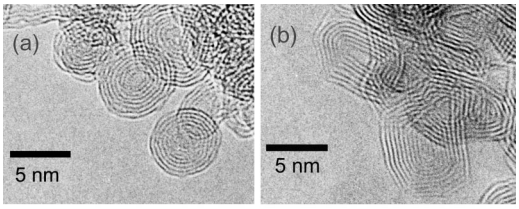

FIG. 1. TEM images of (a) defective spherical carbon onions and (b) polyhedral carbon onions prepared by annealing diamond nanoparticles. These micrographs have already appeared in our previous paper (Ref. 17).

failed to account for the interstellar feature. As an alternative possible candidate, carbon onions with diamond cores have been proposed.[26] This onion model, however, still contained several discrepancies. Even now a precise onion model that explains well the interstellar features is an open question. The present study may allow us to shed light on an origin of the interstellar extinction feature that is a long-standing important problem in astronomy and astrophysics.

II. ULTRAVIOLET-VISIBLE EXTINCTION SPECTROSCOPY OF CARBON ONIONS

A. Experiments

Samples were prepared by annealing diamond nanoparticles 5 nm in diameter in a high vacuum. Detailed procedures for sample preparation have already been described in our previous paper.[17] The diamond nanoparticles 5 nm in diameter form the onions 5 nm in diameter with narrow size distribution. Diamonds start to be transformed into the onions around 900 °C. Since the transformation proceeds from the surface to the center in each diamond, the onions at the intermediate stage of the transformation have core-shell structures, where shells and cores are graphitic layers and diamonds, respectively.

Spherical carbon onions without diamond cores are formed by annealing at about 1700 °C. Figure 1(a) shows a TEM micrograph of the spherical onions. The ESR experiments for the onions elucidated that the graphitic shells contain a number of structural defects such as dangling bonds.[17] The spherical onions have rather defective structure (a defective spherical onion model) than fullerenelike perfect shells. Very recently, Okotrub *et al.*,[27] based on x-ray emission spectroscopy and quantum-chemical calculation, clarified the presence of defects such as dangling bonds in spherical onions; their results supported our defective spherical onion model. Under the annealing at temperatures higher than 1900 °C, defective spherical onions are further graphitized. This results in the formation of polyhedral onions with facets [Fig. 1(b)]. In the present study, we prepared the samples annealed at temperatures between 900 and 2100 °C. Although not shown here, the TEM images of the low magnification revealed that the onions clump together into much larger cluster. The mean diameter of clusters is assumed to be about 120–140 nm from the catalog specification of initial diamond nanoparticles.

Ultraviolet-visible (UV-Vis.) transmission spectroscopy in the wavelength (λ μm) ranging from 0.2 to 0.6 μm was carried out using double-beam-type spectrometer. Samples were dispersed ultrasonically into the distilled water (about 0.2 mg/cm^3). The water suspension was put into a synthesized quartz cell that is almost transparent in this wavelength region. Another cell filled with only distilled water was used for the reference. The recorded transmittance $[T_{(\lambda)}]$, where $T_{(\lambda)}$ is the transmittance at the wavelength λ, is converted into the extinction $[E_{(\lambda)}]$ by the equation, $E_{(\lambda)} = -\log_{10} T_{(\lambda)}$. All of the experimental extinction spectra were then normalized by using the following equation:[19]

$$NE_{(\lambda)} = [E_{(\lambda)} - E_{(\lambda=0.55)}]/[E_{(\lambda=0.44)} - E_{(\lambda=0.55)}]. \quad (1)$$

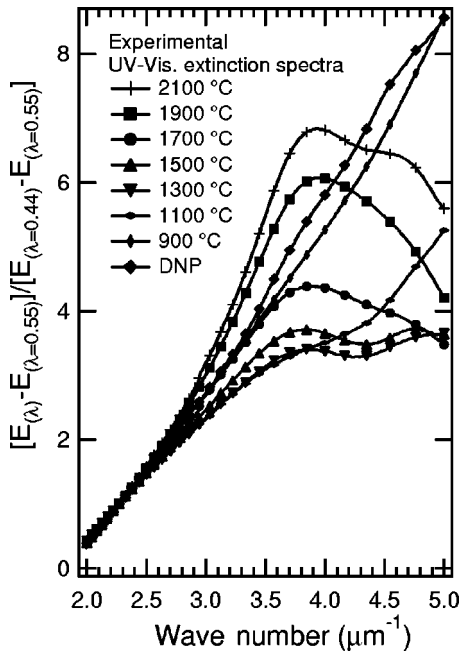

FIG. 2. Experimental UV-Vis. extinction spectra at various annealing temperatures.

B. Ultraviolet-visible extinction spectra

Figure 2 shows experimental UV-Vis. extinction spectra. For convenience, the horizontal axis was converted into the wave number ($1/\lambda$ μm^{-1}). A spectrum for initial diamond nanoparticles denoted by ''DNP'' rises monotonically to the UV region. The monotonic rising extinction continuum cannot be explained by the intrinsic absorption of the diamond, because the band-edge absorption of the bulk diamond normally starts at 4.4 μm^{-1}.

As the annealing temperature increases, the extinction at higher wave numbers decreases. In addition, the sample annealed at 1100 °C shows a broad peak at about 3.7 μm^{-1}. It is worth noticing here that the transformation of diamond nanoparticles into onions starts around 900 °C; defective onions with diamond cores cause the broad peak. At 1700 °C, the peak is more pronounced and slightly shifted to a higher wave number about 3.9 μm^{-1}. TEM studies indicated that, as a result of progress in the transformation, defective spherical onions without diamond cores are formed at this temperature [Fig. 1(a)]. The peak around 3.9 μm^{-1} at 1700 °C is

thus due to the defective spherical onions. With further increasing the annealing temperature, an additional peak at about 4.6 μm^{-1} emerges and a spectrum at 2100 °C exhibits two peaks. The appearance of the two peaks is believed to be associated with the formation of polyhedral onions with facets.

In the next section, we will construct dielectric models of the onions, theoretically consider their extinction properties, and address the following features in the experimental spectra: (i) the rising extinction continuum for initial diamond nanoparticles; (ii) the broad extinction peak at about 3.9 μm^{-1} for defective spherical onions; (iii) the two peaks at 3.9 and 4.6 μm^{-1} for polyhedral onions. Moreover, we attempt to extend our theoretical considerations to the interstellar extinction problem.

III. THEORETICAL CONSIDERATIONS FOR EXTINCTION PROPERTIES OF CARBON ONIONS

A. Absorption of an isolated defective spherical onion

The theoretical scheme for the calculation of absorption spectra of carbon onions with core materials have already been given by Lucas and co-workers.[9,26] The spherical coordinates (unit vectors $\mathbf{r}$, $\boldsymbol{\theta}$, $\boldsymbol{\phi}$) provide the dielectric tensor of graphitic multishell expressed as

$$\epsilon(\omega)=\epsilon_{\perp}(\omega)(\boldsymbol{\theta\theta}+\boldsymbol{\phi\phi})+\epsilon_{\parallel}(\omega)\mathbf{rr}, \tag{2}$$

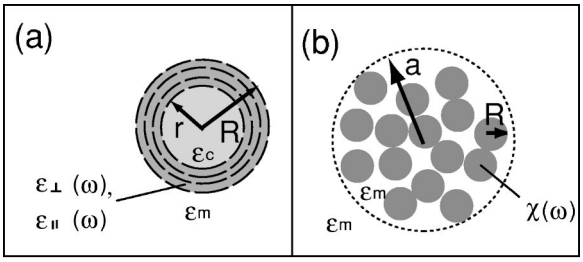

FIG. 3. Schematic illustrations of (a) a defective spherical onion with core material and (b) an aggregate of the onions.

where $\epsilon_{\perp}(\omega)$ and $\epsilon_{\parallel}(\omega)$ are respectively the components of the dielectric tensor at a frequency ω of graphitic shells in the direction perpendicular and parallel to the c axis. As schematically illustrated in Fig. 3(a), the spherical onion is composed of outer graphitic shells with radius R and inner core with radius r. The core, which is empty[9] or filled with diamond,[26] is expressed by an isotropic dielectric constant of ϵ_c.

The electromagnetic response of the onions is described by their polarizability, which is defined as the proportionality coefficient connecting the external applied potential to the induced one.[28] Considering an onion placed in a homogeneous medium having dielectric constant ϵ_m, the multipolar polarizability of order l can be calculated by the following equation:

$$\alpha_l(\omega)=4\pi\epsilon_0 R^{2l+1}\frac{\epsilon_m[(\epsilon_{\parallel}u_- -\epsilon_c l)(\epsilon_{\parallel}u_+ -\epsilon_m l)-\rho_l(\epsilon_{\parallel}u_+ -\epsilon_c l)(\epsilon_{\parallel}u_- -\epsilon_m l)]}{(l\epsilon_c-\epsilon_{\parallel}u_+)[\epsilon_{\parallel}u_- +\epsilon_m(l+1)]\rho_l-(l\epsilon_c-\epsilon_{\parallel}u_-)[\epsilon_{\parallel}u_+ +\epsilon_m(l+1)]}, \tag{3}$$

where ϵ_0 is the permittivity of vacuum, $u_{\pm}=0.5\{-1\pm[1+4l(l+1)\epsilon_{\perp}(\omega)/\epsilon_{\parallel}(\omega)]^{1/2}\}$, and $\rho_l=(r/R)^{u_+-u_-}$. At the nonretarded limit, the electric field of plane-wave electromagnetic radiation only induces an electric dipole with $l=1$, i.e., Fröhlich mode, which absorbs energy from the wave with the cross section $\sigma(\omega)$. The $\sigma(\omega)$ is directly given by the imaginary part of $\alpha_{l=1}(\omega)$ according to

$$\sigma(\omega)=\frac{4\pi\omega}{c}\mathrm{Im}[\alpha_{l=1}(\omega)], \tag{4}$$

where c is the velocity of light.

In the calculation demonstrated by Lucas *et al.*,[9] the dielectric functions of graphitic shells [$\epsilon_{\perp}(\omega)$ and $\epsilon_{\parallel}(\omega)$] were set to those of bulk graphite which depend on the crystallographic orientations [$\epsilon_{g\perp}(\omega)$ and $\epsilon_{g\parallel}(\omega)$] tabulated by Drain and Lee.[29] However, we should recall here that our previous ESR study[17] suggested that the graphitic shells of spherical onions prepared from diamond nanoparticles contain a number of defects. To take the effects of defects into the calculation, the dielectric functions of defective graphite should be used for $\epsilon_{\perp}(\omega)$ and $\epsilon_{\parallel}(\omega)$. Although the dielectric function could be derived accurately using a first-principle approach, such approach for defective graphite has not yet been established. Therefore, in this paper, we simply assume that the anisotropic dielectric functions of defective graphitic shells are the admixtures of dielectric functions of bulk graphite [$\epsilon_{g\perp}(\omega)$ and $\epsilon_{g\parallel}(\omega)$] and that of amorphous carbon [$\epsilon_a(\omega)$] tabulated by Michel *et al.*[30] as follows:

$$\epsilon_{\perp}(\omega)=c_g\epsilon_{g\perp}(\omega)+(1-c_g)\epsilon_a(\omega), \tag{5}$$

$$\epsilon_{\parallel}(\omega)=c_g\epsilon_{g\parallel}(\omega)+(1-c_g)\epsilon_a(\omega), \tag{6}$$

where c_g is the concentration of graphite in the defective graphitic shells. Because the TEM image of defective spherical onions [Fig. 1(a)] shows lattice fringes corresponding to (002) planes of graphite, c_g is considered to be nearly unity; c_g was set to be 0.8 for the defective onions in the present calculations. TEM studies also indicate that the outer radius R of the particles is about 2.5 nm. The transformation from initial diamond nanoparticles into spherical onions via the onions with diamond cores corresponds to changing r from 2.5 to 0.35 nm (r/R from 1 to 0.14) if the smallest shell in the center of the onion has the same radius as C_{60}. Even though it is difficult to determine definitely the parameters c_g

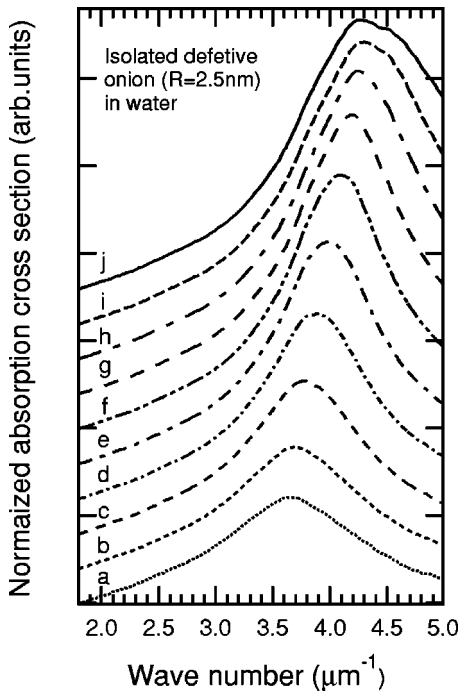

FIG. 4. Calculated absorption spectra for an isolated defective spherical onion ($R=2.5$ nm) in water. The r/R are 0.96 (curve a), 0.9 (b), 0.8 (c), 0.7 (d), 0.6 (e), 0.5 (f), 0.4 (g), 0.3 (h), 0.2 (i), 0.14 (j). For curve j the core is empty, while filled with diamond for curves a to i. The c_g is set to 0.8.

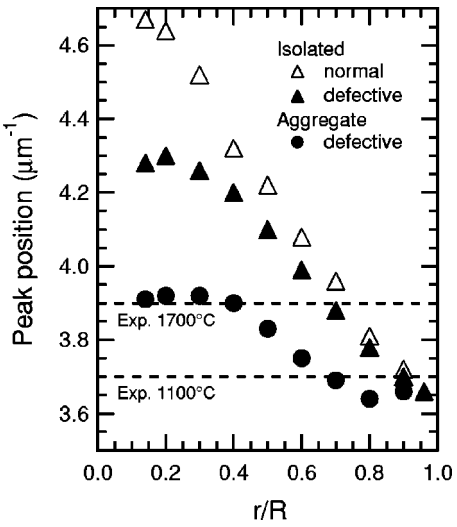

FIG. 5. r/R versus peak positions of the isolated normal spherical onion with $c_g=1$ (open triangle), the isolated defective spherical onion with $c_g=0.8$ (solid triangle), and the aggregate of the defective onions (solid circle) in water medium. The shift variation of experimental spectra is also shown.

and r/R from experiments, we content ourselves with the present choice of the parameters for semiquantitative theoretical considerations.

We can calculate here the absorption cross section for an isolated defective spherical onion with diamond core placed in water medium ($\epsilon_m=1.777$). The dielectric constants of diamond tabulated by Phillip and Taft[31] were used. The absorption cross section was divided by the particle volume (R^3) and normalized by Eq. (1). It should be mentioned first that a computed spectrum for diamond nanoparticles, i.e., $r/R=1$ and the core is diamond, exhibits no absorption. A pure diamond nanoparticle thus cannot explain the rising continuum to the UV region in the experimental spectra up to 1100 °C. Figure 4 shows computed spectra for the isolated defective onions. The normalized spectra were offsetted in the figure. r/R was varied from 0.96 (curve a) to 0.14 (curve j) by changing r from 2.4 to 0.35 nm. For curve a to i the core was filled with diamond while empty for curve j. Curve a, which corresponds to a diamond nanoparticle with thin sp^2 graphitic layer at the initial stage of the graphitization, shows a broad absorption peak due to the surface plasmon at about 3.7 μm^{-1}. As r/R decreases, i.e., as a diamond nanoparticle is transformed into an onion with a diamond core, the peak becomes stronger and sifts to a higher wave number. The complete transformation into a defective onion without diamond core finally leads to the peak at about 4.3 μm^{-1} as shown in curve j.

The peak frequencies obtained from Fig. 4 are plotted as a function of r/R in Fig. 5 (solid triangle). As r/R decreases, the peak shifts from about 3.7 to 4.3 μm^{-1}. For comparison, we also calculated absorption by an isolated spherical onion with $c_g=1$, which is referred as "a normal spherical onion," in water medium and plot the peak frequencies in Fig. 5 (open triangle). It can be clearly seen that, by introducing the defective onion model, the amount of shift in the calculation becomes much smaller. Nevertheless, it is still larger than the shift variation of the experimental spectra. As given in the same figure, the experimental peak shifted from 3.7 to 3.9 μm^{-1} by annealing up to 1700 °C, i.e., by the transformation of diamond nanoparticles into the spherical onions. The residual misfits between calculation and experimental result are believed to be caused by the clustering effect. The aggregation of the onions by van der Waals force is likely to subsist in water suspensions, because the applied ultrasonic dispersion seems to be insufficient to break the adhesion between the particles.[9] TEM micrographs at low magnification indeed showed that the onions clump together in much larger particles. Therefore it is obvious that the aggregation of the defective spherical onions should be taken into account to explain well the experimental results.

B. Extinction by an aggregate of the defective spherical onions

Here we attempt to calculate extinction spectra for the aggregates of defective spherical onions in water medium. As illustrated in Fig. 3(b), since the aggregate (radius a) is composed of the defective spherical onions (radius R) and water, the aggregate is assumed to have an average dielectric function $[\epsilon_{av}(\omega)]$.[32] The average dielectric function can be described within the framework of the effective-medium theory.[9,12] Among various formulation of effective-medium approximation, we adopt the simplest one developed by Maxwell-Garnet.[33] In the Maxwell-Garnet approach, $\epsilon_{av}(\omega)$ is expressed as

$$\epsilon_{av}(\omega)=\epsilon_m\frac{3+2f\chi(\omega)}{3-f\chi(\omega)}, \tag{7}$$

where f is the volume fraction of inclusions and ϵ_m is dielectric constant of the host medium.[34] The inclusions and host medium are respectively the onions and water in the present study. $\chi(\omega)$ is proportional to the polarizability of the onion of order 1 $[\alpha_1(\omega)]$ as follows:

$$\chi(\omega)=\frac{3\alpha_1(\omega)}{4\pi R^3\epsilon_0\epsilon_m}. \tag{8}$$

Assuming the aggregate of the onions as the sphere, the extinction efficiency of the aggregate having $\epsilon_{av}(\omega)$ is calculated in the framework of the Mie theory described in detail in a standard textbook.[8] The extinction cross section (C_{ext}) can be computed by

$$C_{ext}=\frac{2\pi}{k^2}\sum_{n=1}^{\infty}(2n+1)\mathrm{Re}\{a_n+b_n\}, \tag{9}$$

where $k=2\pi N/\lambda$, and a_n and b_n are the Mie coefficients containing the Bessel functions and relative refractive index (N_1/N). N_1 and N are the refractive indices of the Mie sphere and surrounding medium, respectively. The N_1 can be derived directly from ϵ_{av} of the aggregate. Finally, the extinction efficiency follows from $Q_{ext}=C_{ext}/\pi a^2$. In the present calculation, the radius of the aggregate (a) was set to be 60 nm from the catalog specification of initial diamond nanoparticles. Filling factor (f) was set to be of 0.4. The parameters r/R and c_g, i.e., defective onions composing the aggregate, were the same as those in the corresponding spectra in Fig. 4. These parameters are thought to be sufficient for semiquantitative consideration for the aggregation effects of the onions.

Figure 6 shows the calculated extinction spectra for an aggregate of defective spherical onions ($R=2.5$ nm) in water medium. All of the spectra were normalized and then offsetted. Curve a in Fig. 6, which is the spectrum for an aggregate of particles with $r=2.4$ nm of diamond core, shows rising extinction continuum to UV range with a weak shoulder at about 3.7 $\mu\mathrm{m}^{-1}$. This calculated spectrum is very similar to the experimental ones for the samples annealed up to 1100 °C, which correspond to the diamond nanoparticles coated with thin sp^2 graphitic layers.[17] The similarity allows us to suggest that the rising continuum in the experimental spectra at the initial stage of the graphitization is attributed to the Mie scattering by an aggregate of diamond nanoparticles with thin sp^2 graphitic coating.

Figure 6 demonstrates that the transformation from diamond nanoparticles into defective onions in the aggregate is accompanied by an increase in the intensity of the extinction peak at 3.7 $\mu\mathrm{m}^{-1}$ and a slight shift to a higher wave number; the peak finally reaches at 3.9 $\mu\mathrm{m}^{-1}$ in curve j. In Fig. 5, the peak positions obtained from Fig. 6 are plotted as a function of r/R (solid circle). We see that the peak position for the aggregate weakly depends on r/R, leading to a smaller variation with r/R for the aggregate than that for the isolated onion. It is clearly shown in Fig. 5 that the shift of

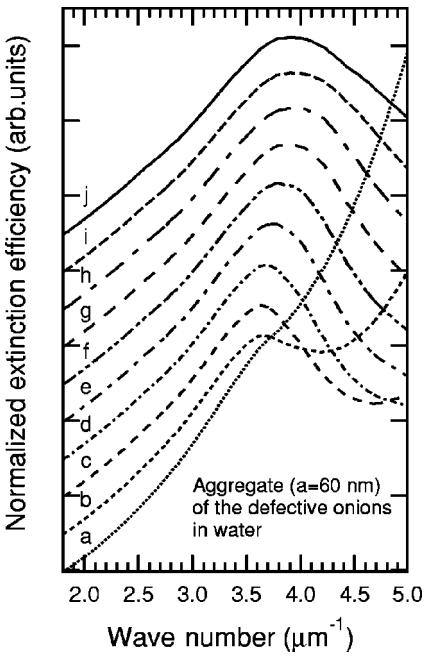

FIG. 6. Calculated extinction spectra for an aggregate ($a=60$ nm) of defective spherical onions in water. The parameters for the defective onions used here are the same ones as in Fig. 4.

the calculated extinction peak for the aggregate agrees with that of experimental ones. The aggregate of defective onions is thus successful in reproducing semiquantitatively the experimental results. These theoretical considerations demonstrate that the optical extinction properties of the spherical onions prepared from diamond nanoparticles can be explained well by the defective spherical onion model.

C. Interstellar extinction features

Let us now extend our theoretical considerations to the extinction spectrum of defective spherical onions in interstellar space. In relation with this astrophysical context, the extinction by an isolated defective onion in vacuum should be considered because the interstellar dust particle with sizes in the 1–20-nm range are usually supposed not to be aggregated. For such nanoparticles, scattering in the UV region is negligible and contribution to the extinction curve is dominated by absorption.[9,8] From Eq. (4), the absorption cross section of an isolated defective onion in vacuum can be obtained by replacing ϵ_m with the dielectric constant of vacuum, i.e., $\epsilon_m=1$.

Solid line in Fig. 7 shows the computed spectrum for a single isolated defective onion in vacuum. The defective onion 2.5 nm in radius has a hollow core 0.35 nm in radius as shown in Fig. 1(a). c_g is set to be 0.8. The computed spectrum successfully reproduces the interstellar extinction curve observed by Savage and Mathis (dashed line).[35] A broad feature between 2–3 $\mu\mathrm{m}^{-1}$ in the observed data is considered to originate from the astronomical silicate. The present results indicate that the defective spherical onions are likely to be an origin of the interstellar extinction bump at 4.6 $\mu\mathrm{m}^{-1}$. Detailed discussion on the interstellar features is beyond the scope of this paper and will appear in the forthcoming report.

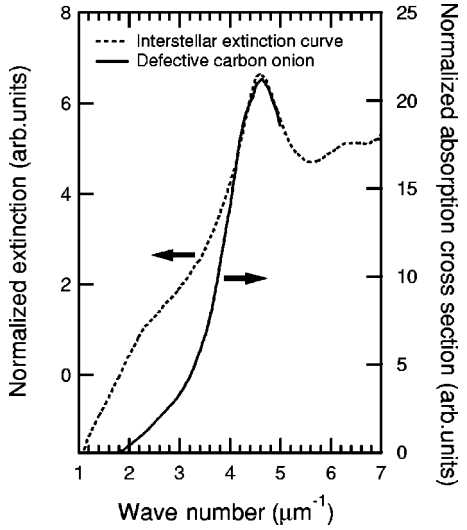

FIG. 7. A normalized computed spectrum for an isolated defective onion in vacuum (solid line) and an observed interstellar extinction curve reported by Savage and Mathis (dashed line) (Ref. 35). The single isolated defective onion 2.5 nm in radius has a hollow core 0.35 nm in radius. The computed spectrum successfully reproduces the interstellar feature at 4.6 μm^{-1}. A weak shoulder between 2 and 3 μm^{-1} in the observed data is considered to originate from the astronomical silicate.

D. Extinction by an aggregate of polyhedral onions

The appearance of two extinction peaks for experimental spectra above 1900 °C in Fig. 2 is apparently attributed to the formation of the aggregate consisting of polyhedral onions with facets. In order to consider the extinction properties of polyhedral onions, we should use a different theoretical scheme from that for spherical onions because the shape effect is not negligible in the surface modes of the particles.[11,36] In this paper, we assume that a polyhedral onion is composed of planar graphite nanocrystals. Such a nanocrystal is treated as an ellipsoidal graphite with crystalline anisotropy as illustrated in Fig. 8(a). Aggregates of polyhedral onions in water are thus modeled as a system consisting of anisotropic graphite nanoellipsoids that are randomly oriented in water [Fig. 8(b)]. We can here adopt a framework of average dielectric function for a medium containing anisotropic ellipsoids developed by Hayashi *et al.*[37] For an ellipsoidal particle, ξ, η, and ζ axes are set. Dielectric functions along each axis are expressed by $\epsilon_\xi(\omega)$, $\epsilon_\eta(\omega)$, and

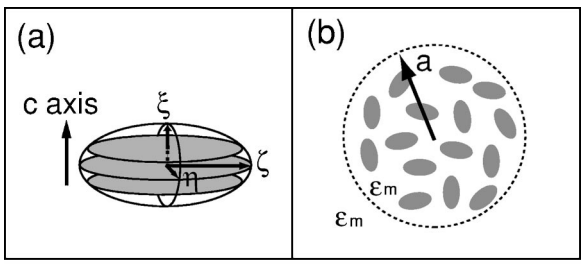

FIG. 8. Schematic illustrations of (a) an ellipsoidal graphite nanocrystal with crystalline anisotropy and the axis configuration, and (b) an aggregate of graphite nanoellipsoids.

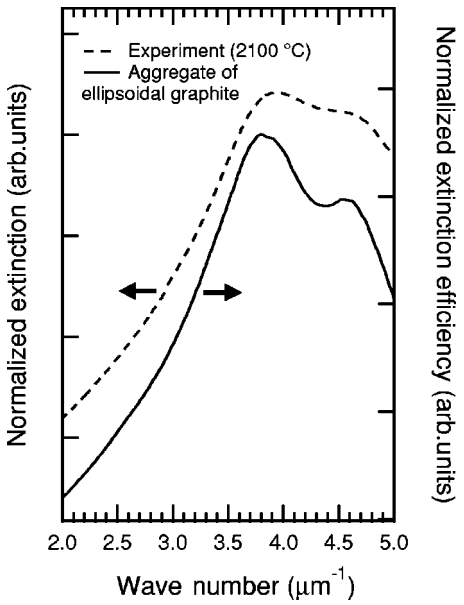

FIG. 9. Solid line represents a computed extinction spectrum for an aggregate of anisotropic ellipsoidal graphite nanocrystals. The aggregate can reproduce successfully the experimental spectrum for polyhedral onions at 2100 °C (dashed line).

$\epsilon_\zeta(\omega)$. Introducing depolarization factors $(L_j, j=\xi,\eta,\zeta)$ along j axis and filling factor (f), the average dielectric function $[\epsilon_{av}(\omega)]$ can be described as[37]

$$\epsilon_{av}(\omega)=1+\frac{3(1-f)(\epsilon_m-1)+f[\widetilde{\epsilon_\xi}(\omega)+\widetilde{\epsilon_\eta}(\omega)+\widetilde{\epsilon_\zeta}(\omega)]}{3(1-f)+f[\widehat{\epsilon_\xi}(\omega)+\widehat{\epsilon_\eta}(\omega)+\widehat{\epsilon_\zeta}(\omega)]}, \tag{10}$$

where

$$\sum_j L_j=1, \quad (j=\xi,\eta,\zeta), \tag{11}$$

$$\widehat{\epsilon_j}(\omega)=[1+L_j[\epsilon_j(\omega)/\epsilon_m-1]]^{-1} \quad (j=\xi,\eta,\zeta), \tag{12}$$

$$\widetilde{\epsilon_j}(\omega)=[\epsilon_j(\omega)-1]\widehat{\epsilon_j}(\omega) \quad (j=\xi,\eta,\zeta). \tag{13}$$

Using $\epsilon_{av}(\omega)$ derived from Eq. (10), the extinction efficiency for an aggregate of graphite ellipsoids can be calculated by the Mie theory. The ξ axis of the ellipsoid is set to parallel to the graphite c axis as shown in Fig. 8(a). $\epsilon_\xi(\omega)$ thus corresponds to $\epsilon_{g\parallel}(\omega)$, while $\epsilon_\eta(\omega)$ and $\epsilon_\zeta(\omega)$ to $\epsilon_{g\perp}(\omega)$. By assuming rotational ellipsoid (spheroid), relations between depolarization factors are described as $L_\xi=L_\eta$ and $2L_\xi+L_\zeta=1$. In the following calculations, L_ζ was set to be 0.1, and thus L_η and L_ξ are 0.45. These depolarization factors correspond to the ratio of the major and minor axes of spheroid of 3.[8] The radius of the aggregate (a) was 60 nm. The filling factor f was set to be of 0.2.

The solid line in Fig. 9 shows a calculated extinction efficiency for an aggregate of graphite ellipsoids in water. The spectrum was normalized by Eq. (1). The calculated spectrum exhibits two peaks at 3.9 and 4.6 μm^{-1}. The double peaks are induced by surface plasmons along η and ζ axes in

the ellipsoid. An experimental extinction spectrum for the polyhedral onions formed at 2100 °C is also shown as dashed line in the same figure. Figure 9 demonstrates that the aggregate of ellipsoidal graphite nanoparticles that we considered here accounts for the experimental results.

IV. CONCLUSIONS

We have studied optical extinction properties of the carbon onions prepared from diamond nanoparticles. Experimental extinction spectra of the spherical and polyhedral onions dispersed in distilled water were acquired by optical transmission spectroscopy. For spherical onions in water, a broad extinction peak emerged around 3.9 μm^{-1}. On the other hand, polyhedral onions showed a spectrum with two peaks at 3.9 and 4.6 μm^{-1}. In order to interpret these experimental results, we carried out semiquantitative theoretical considerations. A new dielectric model, named the defective spherical onion model, was constructed for spherical onions. The calculations demonstrated that the aggregate of the defective spherical onions in water medium explains well the experimental features. The spectrum with double peaks for polyhedral onions can be reproduced successfully by assuming the aggregate of the onions as that of anisotropic graphite nanoellipsoids. In relation with the astrophysical context, the present calculation implies that defective spherical carbon onions are likely candidate for an origin of the interstellar extinction bump at 4.6 μm^{-1}.

ACKNOWLEDGMENTS

Authors would like to acknowledge Yasunori Tsukuda for his valuable contribution to the optical transmission spectroscopy. Acknowledgement is also due to David Tománek and Manish Chhowalla for their fruitful discussions. One of the authors (S.T.) is thankful to the financial support by the Japan Society for the Promotion of Science (JSPS). This work is partially supported by a Grand-in-Aid for Scientific Research from the Ministry of Education, Culture, Sports, Science, and Technology, Japan, and a Grant for Research for the Future Program from the JSPS (JSPS-RFTF-98P-01203).

*Email address: s-tomita@riken.go.jp

[1] H. W. Kroto, J. R. Heath, S. C. O'Brien, R. F. Curl, and R. E. Smalley, Nature (London) **318**, 162 (1985).
[2] D. Ugate, Nature (London) **359**, 707 (1992).
[3] D. Tománek, W. Zhong, and E. Krastev, Phys. Rev. B **48**, 15 461 (1993).
[4] P. Apell, D. Östling, and G. Mukhopadhyay, Solid State Commun. **87**, 219 (1993).
[5] L. Henrard, F. Malengreau, P. Rudolf, K. Hevesi, R. Caudano, Ph. Lambin, and Th. Cabioc'h, Phys. Rev. B **59**, 5832 (1999).
[6] T. Stöckli, J-M. Bonard, A. Châtelain, Z. L. Wang, and P. Stadelmann, Phys. Rev. B **61**, 5751 (2000).
[7] T. Pichler, M. Knupfer, M. S. Golden, J. Fink, and T. Cabioc'h, Phys. Rev. B **63**, 155415 (2001).
[8] C. F. Bohren and D. R. Huffman, *Absorption and Scattering of Light by Small Particles* (John Wiley & Sons, New York, 1983).
[9] A. A. Lucas, L. Henrard, and Ph. Lambin, Phys. Rev. B **49**, 2888 (1994).
[10] W. A. de Heer and D. Ugarte, Chem. Phys. Lett. **207**, 480 (1993).
[11] L. Henrard, P. Senet, Ph. Lambin, and A. A. Lucas, Synth. Met. **77**, 27 (1996).
[12] Th. Cabioc'h, S. Camelio, L. Henrard, and Ph. Lambin, Eur. Phys. J. B **18**, 535 (2000).
[13] S. Tomita, M. Fujii, S. Hayashi, and K. Yamamoto, Chem. Phys. Lett. **305**, 225 (1999).
[14] V. L. Kuznetsov, A. L. Chuvilin, Y. V. Butenko, I. Y. Mal'kov, and V. M. Titov, Chem. Phys. Lett. **222**, 343 (1994).
[15] E. D. Obraztsova, M. Fujii, S. Hayashi, V. L. Kuznetsov, Yu. V. Butenko, and A. L. Chuvilin, Carbon **36**, 821 (1998)
[16] V. L. Kuznetsov, I. L. Zilberberg, Yu. V. Butenko, A. L. Chuvilin, and B. Segall, J. Appl. Phys. **86**, 863 (1999).
[17] S. Tomita, T. Sakurai, H. Ohta, M. Fujii, and S. Hayashi, J. Chem. Phys. **114**, 7477 (2001).
[18] S. Tomita, A. Burian, J. C. Dore, D. LeBolloch, M. Fujii, and S. Hayashi, Carbon **40**, 1469 (2002).
[19] J. S. Mathis, Annu. Rev. Astron. Astrophys. **28**, 37 (1990).
[20] E. L. Fitzpatrick and D. Massa, Astrophys. J., Suppl. Ser. **72**, 163 (1990).
[21] J. S. Mathis, W. Rumpl, and K. H. Nordsiek, Astrophys. J. **217**, 425 (1977).
[22] P. A. Aannestad, Astrophys. J. **443**, 653 (1995).
[23] J. S. Mathis and G. Whiffen, Astrophys. J. **341**, 808 (1989).
[24] J. -M. Perrin and J.-P. Sivan, Astron. Astrophys. **247**, 497 (1981).
[25] E. L. Wright, Astrophys. J. **320**, 818 (1987).
[26] L. Henrard, Ph. Lambin, and A. A. Lucas, Astrophys. J. **487**, 719 (1997).
[27] A. V. Oktrub, L. G. Bulusheva, V. L. Kuznetsov, Yu. V. Butenko, A. L. Chuvilin, and M. I. Heggie, J. Phys. Chem. A **105**, 9781 (2001).
[28] M. Kociak, O. Stéphan, L. Henrard, V. Charbois, A. Rothschild, R. Tenne, and C. Colliex, Phys. Rev. Lett. **87**, 075501 (2001).
[29] B. T. Drain and H. M. Lee, Astrophys. J. **285**, 89 (1984).
[30] B. Michel, Th. Henning, C. Jäger, and U. Kreibig, Carbon **37**, 391 (1999).
[31] H. R. Phillip and E. A. Taft, Phys. Rev. **136**, A1445 (1964).
[32] T. Kozasa, J. Blum, and T. Mukai, Astron. Astrophys. **263**, 423 (1992).
[33] J. C. Maxwell-Garnet, Philos. Trans. R. Soc. London, Ser. A **203**, 385 (1904).
[34] H. G. Craighead and A. M. Glass, Opt. Lett. **6**, 248 (1981).
[35] B. D. Savage and J. S. Mathis, Annu. Rev. Astron. Astrophys. **17**, 73 (1979).
[36] L. Henrard and Ph. Lambin, J. Phys. B **29**, 5127 (1996).
[37] S. Hayashi, N. Nakamori, and H. Kanamori, J. Phys. Soc. Jpn. **46**, 176 (1979).